Toward Estimation of Abnormal Brake in Autonomous Vehicles from Electroencephalogram and Heart Rate Interval

Erika Sekiguchi*, Ken Kubota§, Shun Nakamura*†, Kenichi Makita‡ and Toshihisa Tanaka*
* Tokyo University of Agriculture and Technology, Tokyo, Japan
§ JATCO Engineering Ltd, Shizuoka, Japan
† CorLab Inc., Tokyo, Japan
‡ Innovative Technology Development Department, JATCO Ltd, Shizuoka, Japan
E-mail: sekiguchi20@sip.tuat.ac.jp, tanakat@cc.tuat.ac.jp
Tel/Fax: +81-42-388-7123

***Abstract*—The development of automated driving technology has concentrated on safety aspects such as preventing traffic accidents and not focusing on ride comfort. To realize a reliable technology, it is necessary to consider the ride comfort since automated vehicles use computer control for all operations such as steering wheel and gas pedal. In this paper, we hypothesize that abnormalities in braking timing were reflected in the physiological signals. The abnormal braking timing can be identified from the characteristics of EEG and heartbeat interval. We analyzed the EEG and heart rate intervals of normal and abnormal brake timing created by the simulator to verify the hypothesis. We classified the brake condition by a support vector machine. As a result of using the features of the EEG and heartbeat intervals to discriminate the abnormal brake using a support vector machine, four out of the nine experimental participants achieved an average correct answer rate of more than 80%. Therefore, it was found that the abnormal brake could be estimated from EEG and heartbeat interval features under the presentation of driving videos with different braking timing.**

I. Introduction

There is a lot of research and development on automated driving in the automotive industry. Research on automated driving technology concentrates on safety aspects, such as preventing traffic accidents, and does not focus on ride comfort [1], [2]. Since automated vehicles use computer control for all steering wheel and gas pedal operations, ride comfort must also be considered to achieve reliable technology.

Vertical vibrations and speed fluctuations in the direction of travel have been cited as factors that degrade the ride quality of automobiles, with emergency braking, in particular, causing discomfort for passengers [3], [4]. In order to improve the performance of such ride comfort, it is necessary to have an index that can objectively evaluate the passenger's condition numerically.

The validity of physiological signals has been pointed out as one of the methods to evaluate the psychological state of passengers objectively. In particular, alpha-band brain activity and heart rate intervals are effective as indicators of passenger intentions and changes in psychological state [5], [6]. For alpha-band brain activity, Bi et al. reported that event-related desynchronization (ERD) and event-related synchronization (ERS) in the alpha rhythm could be used to control the left and right directional changes of the vehicle [5]. Regarding heart rate intervals, Kato et al. evaluated changes in the driver's psychological state in response to vehicle vibration using the ratio of low-frequency to high-frequency components of the heart rate interval [6]. Furthermore, Hu et al. confirmed ERD in alpha-band brain activity. They reported an increase in the ratio of low-frequency to high-frequency components in the heartbeat interval when experimental participants felt discomfort or stress due to simulated abnormal brake timing [7]. However, whether these features based on brain activity and heartbeat interval can detect break conditions is unclear.

In this paper, we focused on the fact that abnormalities in brake timing are reflected in the psychological signals and hypothesized that EEG and heart rate features could identify the abnormal brake. Two driving videos with different braking timing were presented to the experimental participants, and EEG and ECG intervals were recorded to test this hypothesis. After that, we used a support vector machine (SVM) of the recorded EEG and ECG features to identify the abnormal brake and evaluated the results.

II. Material and Methods

To measure physiological signals during a normal and an abnormal brake in a simulated autonomous vehicle, the experiment was divided into two phases: Phases 1 and 2. During Phase 1, we created a driving simulation of the autonomous vehicle and measured the normal brake distance of each subject under different scenes of driving simulation. In Phase 2, we created normal and abnormal brake situations of driving simulation using the brake distance recorded in Phase 1.

A. Participants

Eighteen participants (15 males and 3 females) with no cognitive function problems participated in the experiment. All participants had obtained a regular driver's license, and

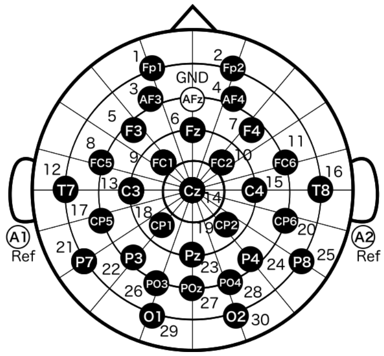

Fig. 1. The electrode locations of EEG

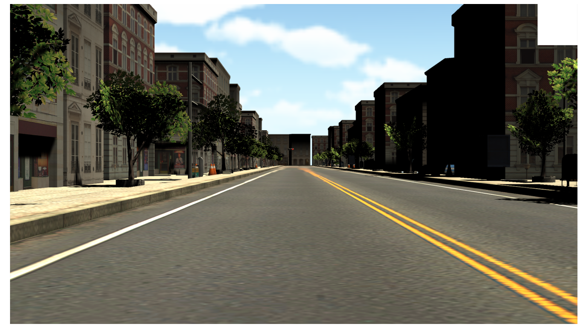

Fig. 2. A screen-shot of a day driving scene

Fig. 3. A photo of the experiment environment and equipment

18 (sub1–sub18) participated in Phase 1. The EEGs of 15 participants were measured, except for sub3, sub6, and sub8. The heart rate intervals of 9 of the 15 participants (sub7, sub9, sub12, sub13, sub14, and sub15; 7 males and 2 females) were measured. Before the experiment, informed consent was obtained from the participants based on the approval of the Research Ethics Committee of Tokyo University of Agriculture and Technology.

B. Data Acquisition

For EEG measurements, 30 scalp electrodes were used according to the electrode configuration of the International 10–20 Method. The electrode configuration can be seen Fig. 1. To confirm eye movements, two electrodes were placed to record the electrooculogram. These observed signals were recorded using a 32-channel DC amplifier (Polymate AP5148, Miyuki Giken, Japan) and software (AP Monitor) with the average of all electrodes as the reference potential. The sampling frequency was set to 1,000 Hz.

The ECG RR interval data was recorded with a wearable heart rate sensor (WHS-1, UNION TOOL Co., Tokyo, Japan). A belt electrode set at the skin below the heart and around the chest was used to record the ECG RR interval.

C. Use Scenes of Driving Simulator

As stimulus materials, we used the driving simulator created by Hu et al. [7], consisting of five city driving scenes as shown in Fig. 2 using Unity 3D (Unity Technologies, USA). We extended the driving scenes to day driving scenes and night driving scenes by changing the lighting environment for a total of ten scenes (five-day and five-night scenes). A signal light and a stop line were provided in each scene, and the vehicle started at an initial speed of 70 kilometers per hour. The total distance from start to stop line was set at 300 m. We used a photodiode to synchronize the stimulus generating machine and the physiological signals recording machine. The white square in the left-upper corner was used to send a signal to the photodiode.

D. Phase 1: Measure Brake Timing

To ensure the normal brake distance that the participant deems appropriate is available. Participants were instructed to focusing on the monitor during the vehicle running and pressed the brake button when they felt they should have brake and the vehicle could stop in front of the stop line smoothly and safely. Unity's program recorded the brake distances. After the participant pressed the brake button, the vehicle decelerated with a constant deceleration and stopped in front of the stop line. One trial consisted of starting and stopping the vehicle, and ten trials were conducted for each scene. As mentioned in the previous section, there were ten different scenes, so 100 trials were conducted. The experiment environment and equipment can be seen in Fig. 3. During the whole experiment, all stimuli were presented on a 31.5-inch LCD monitor. Participants were seated comfortably in a play-seat about 1 m away from the LCD monitor.

E. Phase 2: Measure Physiological Signals

We created auto-driving simulations with two situations: normal and abnormal brake. Using the same brake distance recorded in Phase 1, we created the normal brake auto-driving simulation. Using half of the brake distance recorded in Phase 1, we created the abnormal brake auto-driving simulation. As

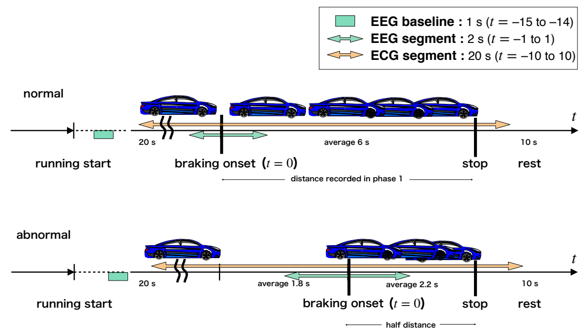

Fig. 4. Phase 2 experiment flow of one trial in normal and abnormal brake situation. The onset of breaking in both conditions is defined as $t = 0$ in the analysis. There were 80 normal and 20 abnormal trials in Phase 2.

can be seen in Fig. 4, when the vehicle arrived at each vertical line location of the normal and abnormal brake situation, a trigger signal was sent to the photodiode. The trigger signals were used to synchronize the brake timing of the two different brake situations. The experiment of Phase 2 contained 100 trials (80 normal and 20 abnormal brakes).

F. Signal Pre-processing

The EEG data were analyzed using the open-source Python program MNE-Python [8]. A 0.2–60 Hz FIR bandpass filter (designed with a hamming window) and a 50 Hz notch filter were applied to the signal. Trials with noticeable artifacts were removed from the analysis. For each trial, a 2-s segment, one second before and after the onset of braking ($-1 \leq t \leq 1$), was extracted. The baseline was defined as the signal with a length of a second between -15 and -14 seconds with respect to the onset of braking ($-15 \leq t \leq -14$).

The ECG RR interval data were analyzed using the open-source Python program hrv-analysis 1.0.4 [9]. The RR interval value was removed (the RR interval was 400 or less, 1,200 or more), and the missing value was linearly interpolated. A 20-s segment, 10 seconds before and after the onset of braking ($-10 \leq t \leq 10$), was extracted for each trial.

G. Feature Extraction

We focused on the fact that abnormalities in braking timing were reflected as discomfort in the EEG and heartbeat interval. The feature values extracted from the EEG and heart rate interval were shown in Table I. Fourteen indices were used as feature values.

The EEG feature extraction was carried out using spectral analysis. First, the power distribution was studied by transforming the EEG into power spectral density (PSD) using a fast Fourier transform (FFT) and using 10-s windows with 50% overlapping windows multiplied by the Hamming function. Second, from each window, the EEG was decomposed into subbands: delta (2–4 Hz), theta (4–8 Hz), alpha (8–12 Hz), beta (12–30 Hz), and gamma (30–40 Hz). Third, the PSD results of each frequency band were normalized (1/f) to obtain there lative PSD of each band to the baseline time period. Finally, the resulting PSD values in each band were averaged to obtain the power spectral features used for classification. The power ratios were obtained from the PSD of each frequency band [10].

TABLE I
EEG AND HEARTBEAT INTERVAL FEATURES

Physiological Signals	Features
EEG	Theta power (4–8 Hz)
	Alpha power (8–13 Hz)
	Low alpha power (8–10 Hz)
	High alpha power (10–13 Hz)
	Beta power (13–30 Hz)
	Low beta power (13–21 Hz)
	High beta power (21–30 Hz)
	Gamma power (30–47 Hz)
	Beta/(Alpha+Theta))
	Theta/Alpha
	Theta/Beta
ECG RR interval	LF/HF ratio
	CSI
	CVI

The RR interval feature extraction was carried out using frequency domain analysis and non-linear domain analysis. For frequency domain analysis, the preprocessed RRI values were linearly interpolated and transformed into power spectral density (PSD) using fast Fourier transform (FFT) to estimate the power distribution. In addition, the low-frequency component (LF, 0.04–0.15 Hz) indicating sympathetic nervous system activity and the high-frequency component (HF, 0.15–0.40 Hz) indicating parasympathetic nervous system activity were calculated. For each epoch, obtained the ratio of LF to HF. For nonlinear domain analysis, the sympathetic index, cardiac sympathetic index (CSI), and the parasympathetic index, cardiac vagal index (CVI), were calculated using a Lorenz plot [11].

H. Classification

The classification task was to estimate normal or abnormal braking based on the psychological signals recorded from each participant. Therefore, we classified it into two classes using Support Vector Machine (SVM).

To measure the classifier's performance, the data was divided into two parts with training and testing and to report performance. k-fold cross-validation ($k = 10$) was performed on the data set; the data set was randomly divided into k partitions. Then, $k - 1$ partitions were used to fit the learning model, and the remaining partition was used to validate the model; this process was repeated k times, and each time using a different partition to validate the model.

III. Results

A. EEG Spectrogram and LF/HF Ratio of Heart Rate Interval

The 2–47 Hz spectrogram of the EEG and the LF/HF ratio of the heartbeat interval were calculated [7]. These results are shown in Figs. 5 and 6.

The EEG spectrograms were averaged over all experimental participant (sub) trials during normal and abnormal conditions.

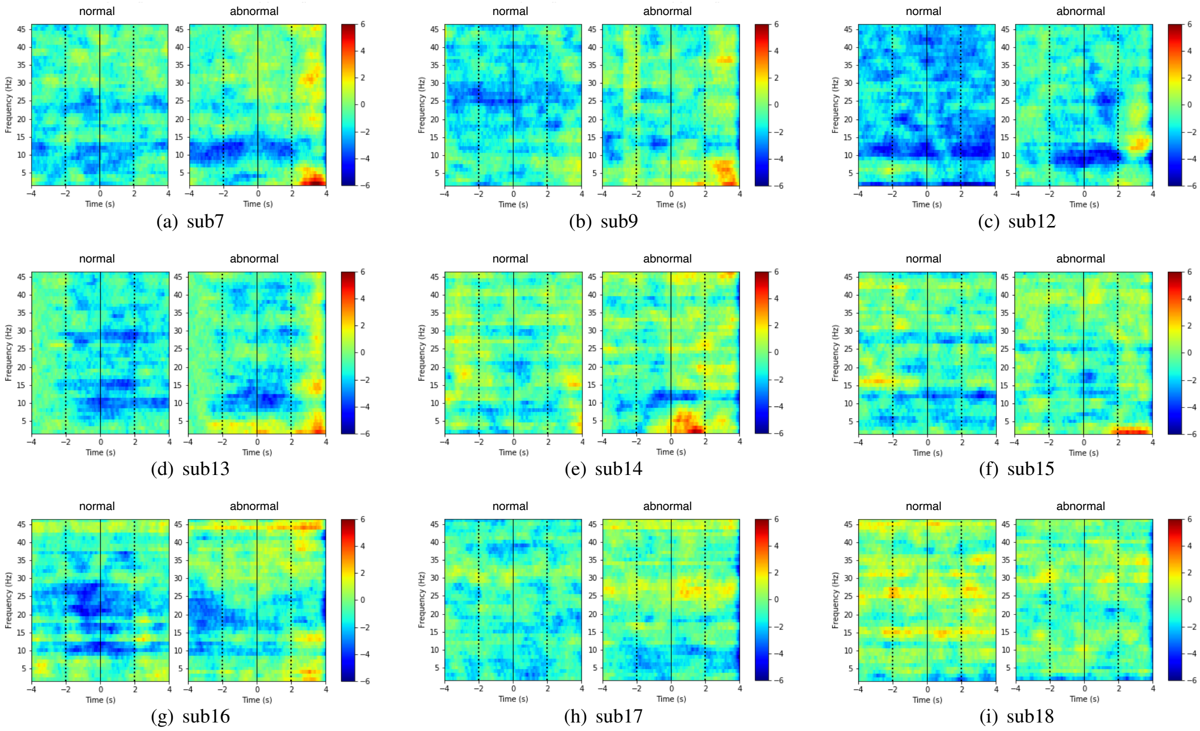

Fig. 5. Spectrograms of normal (left) and abnormal braking (right) are shown for each experimental participant

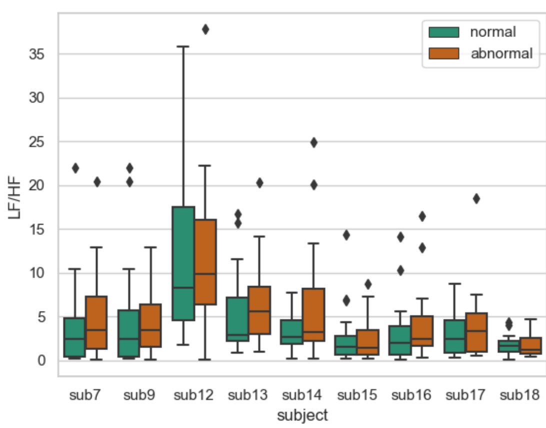

Fig. 6. The LF/HF ratios of the heart rate intervals during normal and abnormal braking are shown in box plots for each participant.

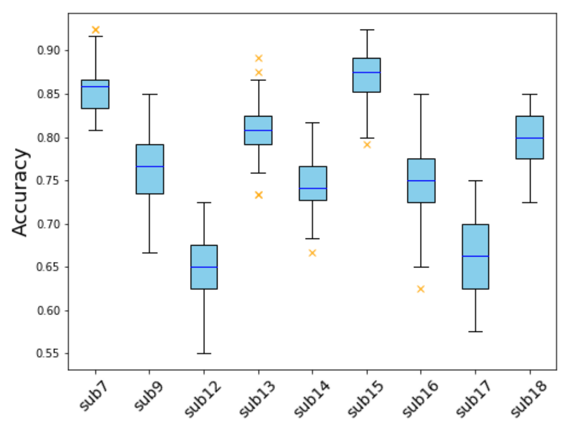

Fig. 7. Average percentage of correct answers for 10-segment cross-validation of SVM

The figure's black vertical line ($t = 0$) indicates the brake timing, and the black dotted line ($t = 2$) indicates the interval used to extract the features. In sub7, sub12, sub13, and sub14, ERD was observed at 8–16 Hz before and after braking ($-2 \leq t \leq 2$), especially during abnormal braking. Furthermore, in sub7, sub9, sub12, sub13, sub14, sub15, and sub16, ERS was observed at 2 to 8 Hz after braking ($0 \leq t \leq 2$) during abnormal braking.

The LF/HF ratio was calculated from the heart rate intervals of each experimental participant (sub) and each trial for normal and abnormal braking, respectively. In sub7, sub12, sub13, sub14, sub16, and sub17, all trials' mean LF/HF ratio was higher during abnormal braking than during normal braking.

B. Estimation of Abnormal Braking with SVM Using EEG and Heart Rate Interval Features as Input

The features calculated from the EEG and heart rate intervals for each trial were used to perform a two-class classification of abnormal braking estimation by SVM. Fig. 7 shows the average accuracy after 50 trials of 10-segment cross-validation within the experimental participants. In the figure, the x-axis shows the participant number, and the y-axis shows the average accuracy. Perfect classification means that the accuracy is equal to 1, and 0.5 means random performance. Of the nine participants in the experiment, four achieved an average accuracy of 80% or higher.

IV. Discussion

A. EEG spectrogram and LF/HF Ratio of Heart Rate Interval

The EEG and heart rate intervals responded differently to normal and abnormal braking. The EEG spectrogram showed that ERD in the alpha band (8–13 Hz) tended to be induced before and after braking ($-2 \leq t \leq 2$), especially during abnormal braking. From the heart rate interval, the ratio of LF to HF tended to be higher during abnormal braking. Local alpha-band (8–12 Hz) ERD is a response to unpleasant emotions [12]. In addition, sympathetic and parasympathetic nervous system activity (degree of tension) can be assessed from the ratio of LF to HF, with a higher LF/HF ratio being associated with mental stress [13], [14]. These studies suggest that the experimental participants felt uncomfortable and stressed in response to the brake abnormality, which induced alpha-band ERD in the EEG and a larger LF/HF ratio in the heartbeat interval. Therefore, it might be possible to estimate abnormal braking by using the differences in the characteristics of these EEG and heartbeat intervals.

B. Estimation of Abnormal Braking with SVM Using EEG and Heart Rate Interval Features as Input

Using the features calculated from the EEG and heartbeat intervals of one trial (Table I), two-class discrimination for abnormal braking estimation was performed by SVM, and four of the nine experimental participants achieved an average correct classification rate of 80% or higher. This suggests that it is possible to estimate the driver's abnormal braking by using the physiological signals before and after the braking timing.

However, the classification results varied among the experimental participants. This may be because single-channel (Pz-electrode) EEG was used for feature extraction. The Pz-electrode did not reflect enough spatial features for discrimination due to the displacement of the head cap during the experiment. Therefore, features should be extracted from multiple electrodes in future studies. For example, the filter-bank common spatial pattern method can be considered [15] and causal relationships between EEG electrodes obtained by multivariate autoregressive models can also be used as features for discrimination [16]. We will investigate these feature extraction methods to discriminate abnormal braking with higher accuracy and study, based on the results obtained in the simulator, applying these features to EEG and heart rate intervals recorded while riding in a real car.

References

[1] K. Jo, J. Kim, D. Kim, C. Jang, and M. Sunwoo, "Development of autonomous car-part i: Distributed system architecture and development process," *IEEE Transactions on Industrial Electronics*, vol. 61, no. 12, pp. 7131–7140, 2014.

[2] N. Kalra and S. M. Paddock, "Driving to safety: How many miles of driving would it take to demonstrate autonomous vehicle reliability?" *Transportation Research Part A: Policy and Practice*, vol. 94, pp. 182–193, 2016.

[3] M. J. Griffin, "Discomfort from feeling vehicle vibration," *Vehicle System Dynamics*, vol. 45, no. 7-8, pp. 679–698, 2007.

[4] K. Ebe and M. J. Griffin, "Qualitative models of seat discomfort including static and dynamic factors," *Ergonomics*, vol. 43, no. 6, pp. 771–790, 2000.

[5] L. Bi, T. He, and X. Fan, "A driver-vehicle interface based on ERD/ERS potentials and alpha rhythm," in *2014 IEEE International Conference on Systems, Man, and Cybernetics (SMC)*, 2014, pp. 1058–1062.

[6] H. Kato, M. Ishida, M. Mashino, and T. Narita, "Proposal of ride comfort control system by psychological state estimation of the driver," *Transactions of the JSME*, vol. 81, no. 832, pp. 15–00 356–15–00 356, 2015.

[7] Y. Hu, S. Nakamura, T. Yamanaka, and T. Tanaka, "Physiological signals responses to normal and abnormal brake events in simulated autonomous car," *2019 Asia-Pacific Signal and Information Processing Association Annual Summit and Conference (APSIPA ASC)*, pp. 736–740, 2019.

[8] A. Gramfort, M. Luessi, E. Larson, D. A. Engemann, D. Strohmeier, C. Brodbeck, R. Goj, M. Jas, T. Brooks, L. Parkkonen, and M. S. Hämäläinen, "MEG and EEG data analysis with MNE-Python," *Frontiers in Neuroscience*, vol. 7, no. 267, pp. 1–13, 2013.

[9] "hrv-analysis 1.0.4," https://pypi.org/project/hrv-analysis/.

[10] R. Fernandez Rojas, E. Debie, J. Fidock, M. Barlow, K. Kasmarik, S. Anavatti, M. Garratt, and H. Abbass, "Electroencephalographic workload indicators during teleoperation of an unmanned aerial vehicle shepherding a swarm of unmanned ground vehicles in contested environments," *Frontiers in Neuroscience*, vol. 14, p. 40, 2020.

[11] W. Wang, Y. Wei, N. Guan, and Y. Wang, "The automatic detection and analysis of electrocardiogram based on lorenz plot," pp. 644–649, 2015.

[12] A. C. Atencio, T. F. B. Filho, A. Ferreira, and A. B. Benevides, "Evaluation of ERD/ERS caused by unpleasant sounds to be applied in BCIs," *ISSNIP Biosignals and Biorobotics Conference, BRC*, vol. 4, 2013.

[13] N. Hjortskov, D. Rissén, A. K. Blangsted, N. Fallentin, U. Lundberg, and K. Søgaard, "The effect of mental stress on heart rate variability and blood pressure during computer work." *European journal of applied physiology*, vol. 92, no. 1-2, pp. 84–9, 2004.

[14] F. Shaffer, R. McCraty, and C. L. Zerr, "A healthy heart is not a metronome: an integrative review of the heart's anatomy and heart rate variability," *Frontiers in Psychology*, vol. 5, p. 1040, 2014.

[15] Y. Park and W. Chung, "Selective feature generation method based on time domain parameters and correlation coefficients for filter-bank-csp bci systems," *Sensors*, vol. 19, no. 17, 2019. [Online]. Available: https://www.mdpi.com/1424-8220/19/17/3769

[16] H. Zhang, R. Chavarriaga, M. K. Goel, L. Gheorghe, and J. d. R. Millán, "Improved recognition of error related potentials through the use of brain connectivity features," *2012 Annual International Conference of the IEEE Engineering in Medicine and Biology Society*, pp. 6740–6743, 2012.